Approximation-Free Control for Vehicle Active Suspensions With Hydraulic Actuator

Yingbo Huang, Jing Na, *Member, IEEE*, Xing Wu, and Guanbin Gao

***Abstract*—This paper presents a novel control strategy for nonlinear uncertain vehicle active suspension systems without using any function approximators [e.g., neural networks (NNs) or fuzzy logic systems (FLSs)]. Unlike previous results that neglect the effect of actuator dynamics, this paper incorporates the dynamics of a hydraulic actuator that is used to create the required active suspension forces into the controller design. To address the nonlinearities of this hydraulic system, an approximation-free control method is introduced. In this method, the widely used NNs and FLSs are not needed. This leads to reduced computational burden and complexity, and thus, it is more suited for practical applications. Moreover, by introducing a prescribed performance function and the associated error transform, the proposed controller can guarantee both the transient and steady-state suspension responses. The stability of the closed-loop system and the suspension performance requirements are rigorously proved. Finally, comparative simulations are conducted to validate the improved performance and robustness of the proposed method.**

***Index Terms*—Active suspension control, approximation-free control (AFC), prescribed performance, vehicle suspension systems.**

I. Introduction

TO MEET the ever-increasing passenger comfort and driving safety demand imposed on the automotive industry, considerable research work has been carried out toward the design and control of vehicle suspension systems in the past few decades [1]–[3]. This is because the suspension systems are responsible for transmitting and filtering all forces between the vehicle and the road, and thereby mainly governing the ride comfort and safety. Specifically, since active suspensions are able to add and dissipate energy from systems by using extra actuators placed between the vehicle body and the wheel-axle, a better suspension response can be achieved in comparison to passive suspensions. Hence, research on active suspensions has drawn significant attention in the field, and many advanced control methodologies have been proposed for active suspensions [4]–[6], e.g., backstepping control [7], H_∞/H_2 control [8], adaptive control [5], etc. However, it is noted that all of these control strategies assume that the actuator used in the active suspension systems is an ideal force generator, where the effects of actuator dynamics are neglected. Although elegant simulation results were reported based on this stringent assumption, the inevitable inaccuracy of these controller deigns neglecting actuator dynamics may severely limit their practical application. In fact, the actuator is a dominant component in the active suspension systems to create the required forces to reduce the uninterrupted road roughness.

Typically, in wider operation scenarios of active suspension systems, hydraulic actuators are widely adopted to generate forces to absorb vibrations from the road to the passengers [9], [10]. However, one of the well-known drawbacks of the hydraulic systems is that their highly nonlinear property, which will result in complexity and difficulty in the modeling and controller designs. To tackle this problem, adaptive control with function approximations [e.g., neural networks (NNs) [11] and fuzzy logic systems (FLSs) [12] has been proved as a powerful tool, where the lumped nonlinearities can be approximated by NNs or FLSs. Owing to nice function approximation ability of NNs or FLSs, the nonlinear uncertainties in the active suspension systems can be handled in the controller design, while the suspension performance can be proved. Although satisfactory results have been obtained [11], [12], a critical problem, the computational burden associated with NNs and FLSs, has not been fully resolved, and only semiglobal stability can be proved. This fact creates difficulties in applying such function approximation based adaptive control methods in practical suspension systems. Thus, it deserves to exploit new control strategies without using function approximations.

On the other hand, from the perspective of practical application in vehicles, the potential poor transient response (e.g., overshoot, sluggish convergence) of the aforementioned control methods may result in performance degradation, hazards, and even cause hardware damage. To guarantee the transient control performance, Bechlioulis and Rovithakis originally proposed a novel controller design and synthesis methodology [13]. This method guarantees that both the transient and steady-state control performance can be analytically examined and prescribed by introducing a prescribed performance function (PPF) and a coordinate error transform. This idea has also been further tailored for strict-feedback systems [14], servo mechanisms [15], and

Manuscript received July 7, 2017; revised October 24, 2017 and December 25, 2017; accepted January 14, 2018. Date of publication January 26, 2018; date of current version May 1, 2018. This work was supported in part by the National Natural Science Foundation of China (NSFC) under Grant 61573174, and in part by a joint grant between NSFC and Royal Society of U.K. under Grant IE150833/61611130213. *(Corresponding author: Jing Na.)*

The authors are with the Faculty of Mechanical and Electrical Engineering, Kunming University of Science and Technology, Kunming 650500, China (e-mail: Yingbo_Huang@126.com; najing25@163.com; xingwu@aliyun.com; gbgao@163.com).

Color versions of one or more of the figures in this paper are available online at http://ieeexplore.ieee.org.

Digital Object Identifier 10.1109/TIE.2018.2798564

active suspension systems [5]. However, in all above-mentioned results with PPF, function approximators (e.g., NNs or FLSs) must be used together with adaptive control to tackle unknown system dynamics. Very recently, an approximation-free control (AFC) method was proposed [16] for pure-feedback systems, which can significantly reduce computational burdens because NNs and FLSs are not required. However, this idea has not been studied for active suspension systems.

With the aim to develop a simple yet robust control for active suspension systems, this paper will study an AFC strategy for vehicle active suspension systems with hydraulic actuators and nonlinear dynamics. One salient feature of the controller to be presented lies in that it can not only accommodate modeling uncertainties and nonlinearities without using any function approximators [11], [17], [18] but also guarantee both the transient and steady-state suspension performance. Compared with the aforementioned results with function approximations, where sufficiently large number of NN nodes is needed to approximate the uncertain dynamics, the computational costs of the proposed AFC are significantly reduced. Therefore, this control is suitable for practical application due to its simplicity. We first incorporate the hydraulic actuator into the active suspension system to cover more realistic cases. Then a PPF and the associated error transform are introduced to construct a systematic recursive design procedure for active suspension systems. This transformed error is then used in the controller design, where the finally derived controller has a simple proportional-like structure. The closed-loop system stability is rigorously proved in terms of the initial value problem and Lyapunov theory. Finally, simulations based on a quarter-car active suspension system with hydraulic actuator built in a combined simulator with Carsim 8.1 and MATLAB Simulink are carried out to show the effectiveness of the proposed AFC.

The main contributions can be summarized as follows.

1) An AFC method is proposed for active suspension systems with hydraulic actuators, where function approximations are not used even in the presence of uncertainties, unknown nonlinearities, and disturbances.
2) The developed control can not only achieve reduced computational burdens but also guarantee a predefined suspension response (e.g., displacement convergence rate, overshoot, and maximum steady-state error).

II. Problem Formulation and Preliminaries

A. Dynamic of a Quarter-Car System

This paper will study a quarter-car with nonlinear active suspension system, which is shown in Fig. 1. The definition of all variables used in Fig. 1 is given as m_s is the sprung mass and m_u is the unsprung mass, which refer to the car chassis and the mass of the wheel assembly, respectively; F_d and F_s are the forces produced by the dampers and springs. F_t and F_b denote the elasticity and damping forces of the tire; z_s and z_u are the displacement of sprung and unsprung masses, respectively; z_r is the road displacement input, and F is the force used to eliminate the vertical motion due to the road roughness injected into the suspension system. The forces produced by the springs,

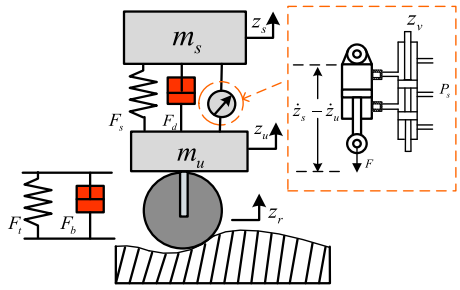

Fig. 1. Active suspension system for a quarter-car with hydraulic actuator.

dampers, and tire are related to the motions of the sprung mass, unsprung mass, and tire.

The mathematical model of the active suspension system shown in Fig. 1 is obtained as [19], [20]

$$\begin{cases} m_s\ddot{z}_s \;+F_d(\dot{z}_s,\dot{z}_u)+F_s(z_s,z_u)=F \\ m_u\ddot{z}_u \;-F_d(\dot{z}_s,\dot{z}_u)-F_s(z_s,z_u)+F_t(z_u,z_r) \\ \qquad\quad +F_b(\dot{z}_u,\dot{z}_r)=-F \end{cases}. \tag{1}$$

In this paper, the dynamics of the actuator used to create the required force F are explicitly considered, i.e., F is generated by a hydraulic actuator placed parallel to the suspension spring and damper, as shown in Fig. 1. In general, the generated force F can be described as $F = A \cdot P_L$, where A is the piston area and P_L is the cylinder's load pressure, which can be directly observed from a pressure gauge. As explained in the literature [21]–[23], a widely used four-way valve-piston actuator is considered in this paper, whose dynamics are expressed as

$$\frac{V_t}{4\beta_e}\dot{P}_L = Q - C_{tp}P_L - A(\dot{z}_s - \dot{z}_u) \tag{2}$$

where V_t is the total actuator volume, β_e is the effective bulk modulus, and C_{tp} is the total piston leakage coefficient. Q is the load flow, which can be calculated as

$$Q = \operatorname{sgn}\left[P_S - \operatorname{sgn}(z_v)P_L\right] C_d\omega z_v \sqrt{\left|P_s - \operatorname{sgn}(z_v)P_L\right|/\rho} \tag{3}$$

where P_s and ρ are the hydraulic supply pressure and fluid density, respectively. C_d is the discharge coefficient, ω denotes the spool valve area gradient, and z_v is the displacement of the spool valve.

In practical hydraulic actuator operations, the valve displacement z_v can be manipulated by a voltage or current input u in corresponding to different required forces. The dynamics of the servo valve can be approximated as [19]

$$\dot{z}_v = \frac{1}{\tau}(-z_v + u) \tag{4}$$

where τ is the time constant of the valve dynamics, and u is the voltage or current input. It is noted that the spool valve dynamics converges much faster than the actuator dynamics as the time constant τ is small. Hence, as validated in [24], (4) can be simplified as an algebraic equation $-z_v + u = 0$. In this case, we can reformulate (2) as

$$\dot{F} = -\beta F - \alpha A^2(\dot{z}_s - \dot{z}_u) + A\gamma u\omega_3 \tag{5}$$

where

$$\beta = aC_{tp}, \quad a = 4\beta_e/V_t, \quad \gamma = aC_d\omega\sqrt{1/\rho}$$
$$\omega_3 = \operatorname{sgn}\left[P_s - \operatorname{sgn}(u)P_L\right]\sqrt{\left|P_s - \operatorname{sgn}(u)P_L\right|/\rho}. \quad (6)$$

To derive a state-space form for the quarter-car active suspension system with hydraulic actuator, we define the state variables as $x_1 = z_s, x_2 = \dot{z}_s, x_3 = z_u, x_4 = \dot{z}_u, x_5 = \mu P_L$, where μ is a positive constant that is chosen to scale the load pressure P_L. Then the dynamics of (1) along (5) can be represented as

$$\begin{cases} \dot{x}_1 = x_2 \\ \dot{x}_2 = \frac{1}{m_s}\left(-F_d(x_2, x_4) - F_s(x_1, x_3) + \frac{A}{\mu}x_5\right) + d_1 \\ \dot{x}_3 = x_4 \\ \dot{x}_4 = \frac{1}{m_u}\left(F_d(x_2, x_4) + F_s(x_1, x_3) - F_t(x_3, z_r)\right. \\ \qquad \left. -F_b(x_4, \dot{z}_r) - \frac{A}{\mu}x_5\right) + d_2 \\ \dot{x}_5 = -\beta x_5 - \mu a A(x_2 - x_4) + \mu\gamma u\omega_3 \end{cases} \quad (7)$$

where the extra bounded terms $|d_i| < d_m, \quad i = 1, 2$ denote the effect of sensor noise, external disturbances, and modeling uncertainties. In addition, the fact $\theta_{\min} \le 1/m_s \le \theta_{\max}$ holds for bounded positive constants $\theta_{\min}$ and $\theta_{\max}$.

In the following controller design and implementation, only the vertical motion displacement and velocity (e.g., $z_s, \dot{z}_s$) and the cylinder's load pressure P_L are used, which can be measured using sensors (e.g., accelerometers, pressure gauge). Moreover, as aforementioned, the controller output u (voltage applied on the servo valve) is the input for the hydraulic system (5), which is used to create the required force F. This generated force F is used to drive the motion of suspension system (1).

Remark 1: In most available results (e.g., [4]–[6]) for active suspension controller designs, the actuators are considered as an ideal force generator. Although satisfactory simulation results have been reported, the practically unavoidable nonlinear behavior of actuators is not considered, which may limit their applications. In contrary, this paper addresses active suspension controller design with a hydraulic actuator to cover realistic cases.

Remark 2: To address nonlinearities of the hydraulic systems, adaptive control with NNs or FLSs has been proposed, e.g., [11], [17], [18]. These approximation-based controls require heavy computational costs and may lead to a sluggish response. This fact motivates us to propose a simple control strategy without using any function approximators even in the presence of modeling uncertainties and hydraulic nonlinearities.

Remark 3: Although most available active suspension control results can guarantee a steady-state performance of the vehicle body displacement, i.e., $x_1 \to 0$, a few number of works have been done to address transient suspension performance. It is clear that the transient suspension response is also crucial, because aggressive or sluggish transient response may trigger suspension performance degradation and even cause damages of suspension components. Hence, in this paper, a new control strategy will be presented to guarantee both the transient and steady-state performance, simultaneously.

B. Prescribed Performance Function

To prescribe the convergence rate, maximum overshoot, and steady-state error of x_1, we introduce the following positive decreasing function $\varphi_i(t) : R^+ \to R^+$ as the PPF [13]–[15]:

$$\varphi_i(t) = (\varphi_{i0} - \varphi_{i\infty})e^{-\alpha_i t} + \varphi_{i\infty}, \quad i = 1 \ldots n \quad (8)$$

where $\varphi_{i0} > \varphi_{i\infty} > 0$ and $\alpha_i > 0$ are the positive parameters, which determine the initial value, ultimate error boundary, and convergence rate, respectively. $\varphi_i(t)$ satisfies the following conditions:

1) $\varphi_i(0) = (\varphi_{i0} - \varphi_{i\infty})e^{-a_i \cdot 0} + \varphi_{i\infty} = \varphi_{i0}$;
2) $\lim_{t\to 0}\varphi_i(0) = \varphi_{i0}, \lim_{t\to+\infty}\varphi_i(t) = \varphi_{i\infty}$.

Thus, the vertical motion can be attenuated by retaining x_i within a prescribed bound, which can be given as

$$-\underline{\delta}\varphi_i(t) < x_i(t) < \bar{\delta}\varphi_i(t) \quad \forall t > 0 \quad (9)$$

where $\underline{\delta}, \bar{\delta}$ are positive constants chosen by the designers.

In (8) and (9), we know that $-\underline{\delta}\varphi_i(0)$ and $\bar{\delta}\varphi_i(0)$ refer to the lower bound of an undershoot and the upper bound of an overshoot. The decreasing rate α_i defines the convergence speed and $\varphi_{i\infty}$ denotes the allowable steady-state error [15]. Thus, both the transient and steady-state performance can be designed *a priori* by tuning parameters $\underline{\delta}, \bar{\delta}, \alpha_i, \varphi_{i0}$, and $\varphi_{i\infty}$.

We will design a controller such that (9) can be guaranteed for all time. The basic idea of the following developments is to transform the control problem of (7) with constraint (9) into an equivalent "unconstrained" control problem as [13]. For this purpose, we define a smooth and strictly monotonic increasing function $S(\zeta_i)$ of the transformed error $\zeta_i(t) \in R$, such that

1) $-\underline{\delta} < S(\zeta_i) < \bar{\delta} \quad \forall\zeta_i \in L_\infty$
2) $\lim_{\zeta_i\to+\infty} S(\zeta_i) = \bar{\delta}, \quad \lim_{\zeta_i\to-\infty} S(\zeta_i) = -\underline{\delta}$.

In this paper, we choose the function $S(\zeta_i)$ as

$$S(\zeta_i) = \frac{\bar{\delta}e^{\zeta_i} - \underline{\delta}e^{-\zeta_i}}{e^{\zeta_i} + e^{-\zeta_i}}. \quad (10)$$

Clearly, we can verify that the inverse function of (10) exists and can be given as

$$\varepsilon_i = S^{-1}[\zeta_i] = \frac{1}{2}\ln\left(\frac{\underline{\delta} + \zeta_i}{\bar{\delta} - \zeta_i}\right). \quad (11)$$

C. Preliminaries

Consider the following initial value problem [25]

$$\dot{\zeta}(t) = \nu(t, \zeta), \quad \zeta(0) = \zeta^0 \in \Omega_\zeta \quad (12)$$

where $\nu : R_+ \times \Omega_\zeta \to R^n$ is a continuous function vector and $\Omega_\zeta \in R^n$ is a nonempty open set.

Definition 1: [25] Any solution $\zeta(t)$ of the initial value problem (12) is maximal if it has no proper right extension that is also a solution of (12).

Theorem 1: [25] For the initial value problem (12), if $\nu(t, \zeta)$ satisfies: a) locally Lipschitz on $\zeta(t)$ for almost all $t > 0$, b) piecewise continuous on t for each fixed $\zeta(t) \in \Omega_\zeta$, and c) locally integrable on t for each fixed $\zeta(t) \in \Omega_\zeta$, then there exists a solution $\zeta(t)$ on the time interval $[0, \tau_{\max})$ with $\tau_{\max} > 0$ such that $\zeta(t) \in \Omega_\zeta$ for $\forall t \in [0, \tau_{\max})$.

Proposition 1: [25] Assume that the conditions of Theorem 1 hold. For a maximal solution $\zeta(t)$ on the time interval $[0, \tau_{\max})$ with $\tau_{\max} < \infty$ and for any compact set $\bar{\Omega}_\zeta \subset \Omega_\zeta$, there exists a time instant $t_1 \in [0, \tau_{\max})$ such that $\zeta(t_1) \notin \bar{\Omega}_\zeta$.

III. Approximation-Free Controller Design

In this section, we will investigate an AFC to regulate the vertical motion x_1 without using any function approximators while guaranteeing both transient and steady-state suspension performance.

A. Controller Design

The governing equations for the vertical motion consist of $\dot{x}_1, \dot{x}_2$, and $\dot{x}_5$, whose dynamics have been defined in (7). It is noted that suspension system (7) is in a strict-feedback form. Generally, for such systems, the most commonly used method is a backstepping control strategy [7]. However, one of its well-known drawbacks is that the high-order derivatives of the virtual control actions must be calculated repeatedly. This leads to the so-called "explosion of complexity" problem and potential peak in the transient stage. To deal with this problem, we will propose a new control strategy that follows a similar recursive procedure to backstepping approaches but with fairly reduced complexity.

Step 1: Define the output error to be minimized as $x_1(t)$. Then the transformed error can be obtained as

$$\varepsilon_1(t) = S^{-1}(\zeta_1(t)) \tag{13}$$

where $\zeta_1(t) = e_1(t)/\varphi_1(t)$ with $e_1(t) = x_1(t)$ is the normalized output error by using a similar PPF defined in (8) as

$$\varphi_1(t) = (\varphi_{10} - \varphi_{1\infty})e^{-\alpha_1 t} + \varphi_{1\infty} \tag{14}$$

where $\varphi_{10}, \varphi_{1\infty}$, and α_1 are positive constants and φ_{10} should be set to fulfill $|x_1(0)| < \min\{\underline{\delta}, \bar{\delta}\}\varphi_{10}$. In this case, one may verify from (11) and (13) that

$$\varepsilon_1 = S^{-1}[\zeta_1] = \frac{1}{2}\ln\left(\frac{\underline{\delta} + \zeta_1}{\bar{\delta} - \zeta_1}\right). \tag{15}$$

Now, we can design an intermediate controller as

$$u_1 = -k_1\varepsilon_1 = -\frac{k_1}{2}\ln\left(\frac{\underline{\delta} + \zeta_1}{\bar{\delta} - \zeta_1}\right) \tag{16}$$

where $k_1 > 0$ is a positive constant control gain.

Step 2: We define the intermediate controller error as

$$e_2(t) = x_2(t) - u_1(t). \tag{17}$$

Then the second transformed error can be obtained as

$$\varepsilon_2(t) = S^{-1}(\zeta_2(t)) \tag{18}$$

where $\zeta_2(t) = e_2(t)/\varphi_2(t)$ is the normalized error with $\varphi_2(t)$ being a PPF given as

$$\varphi_2(t) = (\varphi_{20} - \varphi_{2\infty})e^{-\alpha_2 t} + \varphi_{2\infty} \tag{19}$$

where $\varphi_{20}, \varphi_{2\infty}$, and α_2 are positive constants and φ_{20} is set to fulfill $|e_2(0)| < \min\{\underline{\delta}, \bar{\delta}\}\varphi_{20}$.

Based on (11) and (18), the transformed error of $\zeta_2(t)$ can be derived as

$$\varepsilon_2 = S^{-1}[\zeta_2] = \frac{1}{2}\ln\left(\frac{\underline{\delta} + \zeta_2}{\bar{\delta} - \zeta_2}\right). \tag{20}$$

Hence, another intermediate controller u_2 can be given as

$$u_2 = -k_2\varepsilon_2 = -\frac{k_2}{2}\ln\left(\frac{\underline{\delta} + \zeta_2}{\bar{\delta} - \zeta_2}\right) \tag{21}$$

where $k_2 > 0$ is a positive constant control gain.

Step 3: Similar to Steps 1 and 2, we define the final intermediate controller error as

$$e_3 = x_5(t) - u_2(t). \tag{22}$$

The normalized error $\zeta_3(t) = e_3(t)/\varphi_3(t)$ can be defined with $\varphi_3(t)$ being a PPF given as

$$\varphi_3(t) = (\varphi_{30} - \varphi_{3\infty})e^{-\alpha_3 t} + \varphi_{3\infty} \tag{23}$$

where $\varphi_{30}, \varphi_{3\infty}$, and α_3 are positive constants and φ_{30} should be chosen to fulfill $|e_3(0)| < \min\{\underline{\delta}, \bar{\delta}\}\varphi_{30}$.

From (11), the transformed error ε_3 of $\zeta_3(t)$ is defined as

$$\varepsilon_3 = S^{-1}[\zeta_3] = \frac{1}{2}\ln\left(\frac{\underline{\delta} + \zeta_3}{\bar{\delta} - \zeta_3}\right). \tag{24}$$

Finally, we can design the realistic control input as

$$u = -k_3\varepsilon_3 = -\frac{k_3}{2}\ln\left(\frac{\underline{\delta} + \zeta_3}{\bar{\delta} - \zeta_3}\right) \tag{25}$$

where $k_3 > 0$ is a positive constant control gain.

Remark 4: Compared to the backstepping approach, the derived control actions (16), (21), and (25) are proportional-like controls with the normalized errors $\zeta_i(t)$ and the transformed errors $\varepsilon_i = S^{-1}(\zeta_i)$. Thus, the proposed control strategy is simpler than those obtained from the backstepping procedure [7]. Another salient feature of the proposed control is that no *a priori* knowledge of the system nonlinearities or their upper bounds is required. Furthermore, the widely used function approximators (i.e., NNs, FLSs) are not used in this control implementation. Consequently, the potentially sluggish online learning in [11], [17], and [18] can be remedied, which makes the proposed control implementation attractive.

Remark 5: As indicated before, only a few parameters need to be adjusted in the controller design and implementation. The parameters used in the proposed AFC method can be grouped into two categories: PPF parameters (i.e., $\underline{\delta}, \bar{\delta}, \varphi_{i0}, a_i$, and $\varphi_{i\infty}$) and control gains k_i. The only requirement on the selection of constants $\underline{\delta}, \bar{\delta}$ and φ_{i0} is that they should be chosen to ensure the initial conditions $-\underline{\delta}\varphi_i(0) < e_i(0) < \bar{\delta}\varphi_i(0)$. The convergence speed α_i can be set small at the beginning and then adjusted large by using a trial-and-error method. The steady-state error bound $\varphi_{i\infty}$ can be set large in the initial tuning phase and then reduced subsequently. In general, small $\varphi_{i\infty}$ and large a_i can help obtain better control performance but may lead to large control actions. The control gains k_i should not be set too large because the required control actions must be bounded.

B. Closed-Loop Stability Analysis

In this section, we will analyze the stability of the closed-loop control system. Before we present the main results of this paper, the following lemma is given.

Lemma 1: Consider the suspension error x_1 and control errors e_i in (17) and (22), if we control the transformed errors ε_i in (15), (20), and (24) to be bounded (i.e., $|\varepsilon_i| \leq \varepsilon_{Mi}$ holds for positive constants $\varepsilon_{Mi} > 0$) by using control actions (16), (21), and (25), then $-\underline{\delta}\varphi_i(t) < e_i(t) < \bar{\delta}\varphi_i(t) \quad \forall t > 0$ can be retained, i.e., the prescribed suspension performance of displacement x_1 can be guaranteed by controlling ε_i to be bounded.

Proof: According to the definition and property of the error transformation function (11), the inverse logarithmic function can be calculated as

$$e^{2\varepsilon_i} = \frac{\underline{\delta} + \zeta_i}{\bar{\delta} - \zeta_i} \tag{26}$$

which implies

$$-\underline{\delta} < \frac{e^{-2\varepsilon_{Mi}}\bar{\delta} - \underline{\delta}}{e^{-2\varepsilon_{Mi}} + 1} \leq \zeta_i(t) \leq \frac{e^{2\varepsilon_{Mi}}\bar{\delta} - \underline{\delta}}{e^{2\varepsilon_{Mi}} + 1} < \bar{\delta}. \tag{27}$$

Hence, based on the definition $\zeta_i(t) = e_i(t)/\rho_i(t)$, one may verify that $-\underline{\delta}\varphi_i(t) < e_i(t) < \bar{\delta}\varphi_i(t), \quad \forall t > 0$ is true. ♢

Lemma 1 indicates that we can control the transformed errors ε_i to be bounded to achieve vertical suspension motion x_1 with prescribed bound (9). This Lemma is the basis for the following stability analysis of the closed-loop system.

Now, we summarize the main results of this paper.

Theorem 2: Consider the vertical motion x_1 in the suspension system (7), we design controllers as (16), (21), and (25) with PPF (8). If the initial conditions $|e_i(0)| < \min\{\underline{\delta}, \bar{\delta}\}\varphi_{i0}$ are fulfilled, then x_1 can be retained within the prescribed bound in (9) and all signals in the closed-loop system are bounded.

Proof: We refer to the Appendix for the detailed proof. ♢

C. Suspension Performance Analysis

In addition to the ride comfort that is the major control objective for vehicle active suspension systems, ride safety is also essential in the control synthesis. Generally, the ride safety can be divided into two aspects: 1) The ratio between the tire dynamic load and the stable load should be less than 1, i.e., $|F_t + F_b|/(m_s + m_u)g < 1$; 2) The suspension movement limitation should be guaranteed by $|z_s - z_u| < z_{\max}$, $z_{\max} = 0.15\,\mathrm{m}$.

For the sake of analysis, the elasticity and damping forces F_t and F_b are modeled in [20] as $F_t(z_u, z_r) = k_t(z_u - z_r)$ and $F_b(\dot{z}_u, \dot{z}_r) = b_t(\dot{z}_u - \dot{z}_r)$, where k_t and b_t are the stiffness and damping coefficients of the tire.

We first show the boundedness of x_3 and x_4 in (7). One can obtain from (7) that

$$\dot{x} = Ax + \omega \tag{28}$$

$$x = \begin{bmatrix} x_3 \\ x_4 \end{bmatrix}, \quad A = \begin{bmatrix} 0 & 1 \\ -\frac{k_t}{m_u} & -\frac{b_t}{m_u} \end{bmatrix},$$

$$\omega = \begin{bmatrix} 0 \\ \frac{1}{m_u}\left(k_t z_r + b_t \dot{z}_r + F_d + F_s - \frac{Ax_5}{\mu}\right) + d_2 \end{bmatrix}. \tag{29}$$

Note the control input u is not explicitly included in (28) of the displacement and velocity of unsprung mass ($x_3 = z_u, x_4 = \dot{z}_u$). Moreover, one can verify that the matrix A defined in (29) is Hurwitz, then there exist positive matrices $P > 0, Q > 0$ so that the Lyapunov equation $A^T P + AP = -Q$ holds. In addition, ω is bounded because the road displacement z_r, damper forces F_d, spring forces F_s, sensor noise d_2, x_5, and m_u are all bounded, i.e., $\|\omega\| \leq \bar{\omega}$ holds for a positive constant $\bar{\omega}$. Select a Lyapunov function as $V = x^T Px$ and its derivative can be calculated along (28) as

$$\begin{aligned} \dot{V} &= x^T(A^T P + AP)x + 2x^T P\omega \\ &\leq -\left[\lambda_{\min}(Q) - \lambda_{\max}(P)/\eta\right]\|x\|^2 + \eta\lambda_{\max}(P)\bar{\omega}^2 \end{aligned} \tag{30}$$

where $\eta > 0$ is a positive design parameter coming from the Young's inequality $ab \leq a^2\eta/2 + b^2/2\eta, \quad \eta > 0$ applied to the term $2x^T P\omega$. For appropriately designed parameter $\eta > \lambda_{\max}(P)/\lambda_{\min}(Q)$, it follows from (30) that $\dot{V} \leq -a_1 V + \beta_1$, where $a_1 = [\lambda_{\min}(Q) - \lambda_{\max}(P)/\eta]/\lambda_{\min}(P)$ and $\beta_1 = \eta\lambda_{\max}(P)\bar{\omega}^2$ are all positive constants. By integrating both sides of $\dot{V}$, we have $V(t) \leq V(0)e^{-\alpha_1 t} + \beta_1/\alpha_1$, which further implies that x_3 and x_4 are all bounded by

$$|x_i(t)| \leq \sqrt{(V(0) + \beta_1/\alpha_1)/\lambda_{\min}(P)}, \quad i = 3, 4. \tag{31}$$

Then the bound of the tire load can be derived by

$$\begin{aligned} |F_t + F_b| &\leq (k_t + b_t)\sqrt{(V(0) + \beta_1/\alpha_1)/\lambda_{\min}(P)} \\ &\quad + k_t\|z_r\|_\infty + \|\dot{z}_r\|_\infty. \end{aligned} \tag{32}$$

The driving safety requirement, i.e., $|F_t + F_b|/(m_s + m_u)g < 1$, can be guaranteed by tuning the parameters η and P such that

$$\begin{aligned} &(k_t + b_t)\sqrt{(V(0) + \beta_1/\alpha_1)/\lambda_{\min}(P)} + k_t\|z_r\|_\infty \\ &\quad + \|\dot{z}_r\|_\infty < (m_s + m_u)g. \end{aligned} \tag{33}$$

Finally, the suspension movement limitation will be studied. Based on Theorem 2, we know that $|x_1| < \min\{\underline{\delta}, \bar{\delta}\}\varphi_{10}$. In this sense, we can obtain the bound of suspension space as

$$\begin{aligned} |x_1 - x_3| &\leq |x_1| + |x_3| \leq \min\left\{\underline{\delta}, \bar{\delta}\right\}\varphi_{10} \\ &\quad + \sqrt{(V(0) + \beta_1/\alpha_1)/\lambda_{\min}(P)}. \end{aligned} \tag{34}$$

If we appropriately tune the PPF parameters $\underline{\delta}, \bar{\delta}, \varphi_{10}$ and the design parameters η and P, the suspension movement limitation can be guaranteed, i.e., $|z_s - z_u| < z_{\max}$. It should be noted that the parameters P and η are used for analysis only; they are not used in the control implementation.

IV. Simulations

In this section, we provide simulations to validate the correctness of theoretical studies and show the efficacy of this new

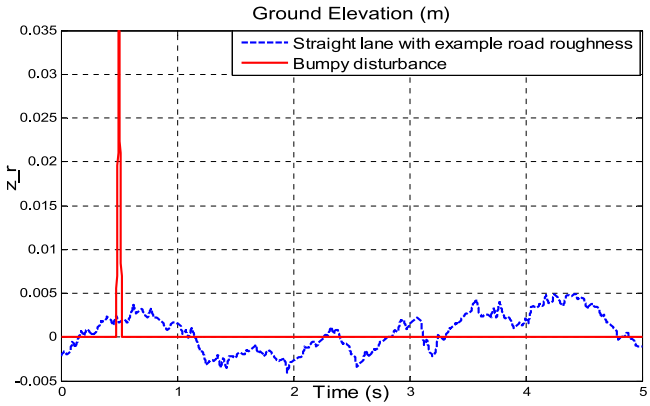

Fig. 2. Ground road elevation.

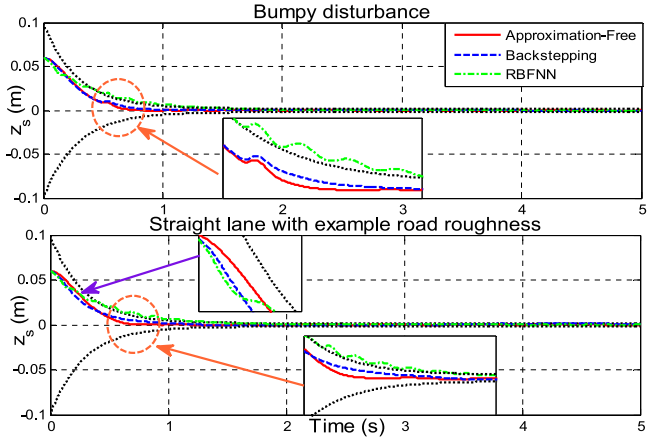

Fig. 3. Vehicle motion with different riding road conditions.

control strategy. For this purpose, a combined simulator built in commercial vehicle simulation software Carsim (Version 8.1) and MATLAB Simulink (2013b) was constructed, which uses realistic vehicle running conditions. It should be noted that the adopted riding road conditions are generated from the Carsim, which come from the experiment data.

The unknown forces of the nonlinear stiffening spring, piecewise damper, and the tire obey are given as [20]

$$F_s(z_s, z_u) = k_s(z_s - z_u) + k_{sn}(z_s - z_u)^3,$$
$$F_d(\dot{z}_s, \dot{z}_u) = b_s(\dot{z}_s - \dot{z}_u)$$
$$F_t(z_u, z_r) = k_t(z_u - z_r), \quad F_b(\dot{z}_u, \dot{z}_r) = b_t(\dot{z}_u - \dot{z}_r) \quad (35)$$

where k_s and k_{sn} are the stiffening coefficients; and b_s is the damping coefficient for the extension and compression movements. k_t and b_t are the stiffness and damping coefficients of the tire. The parameters with respect to the quarter-car model and hydraulic systems are given as [20] $m_s = 600\,\text{kg}, m_u = 60\,\text{kg}, k_s = 18\,000\,\text{N/m}, k_{sn} = 1000\,\text{N/m}, b_s = 2500\,\text{Ns/m}, k_t = 200\,000\,\text{N/m}, b_t = 1000\,\text{Ns/m}, \beta = 1\,\text{s}^{-1}, \mu = 1 \times 10^{-7}, \alpha = 4.151 \times 10^{13}\,\text{N/m}^5, A = 3.35 \times 10^{-4}\,\text{m}^2, r = 1.545 \times 10^9\,\text{N/m}^{5/2} \cdot \text{kg}^{1/2}$, and $P_s = 10\,342\,500\,\text{Pa}$.

In the simulations, two riding road conditions are chosen: a) bumpy road (3.5-cm high, 40-cm long); and b) straight lane with a random roughness road. The ground elevation profiles are plotted in Fig. 2. Furthermore, we set the initial values as $x_1(0) = 0.06\,\text{m}, \quad x_i(0) = 0, \quad i = 2, 3, 4$ and other conditions are set as zero. In road condition a), the PPFs are designed as $\varphi_1(t) = (0.1 - 0.002)e^{-3.5t} + 0.002, \varphi_2(t) = (0.8 - 0.3)e^{-4t} + 0.3, \varphi_3(t) = (1 - 0.1)e^{-10t} + 0.1$ and other parameters are $k_1 = 0.08, k_2 = 1, k_3 = 0.02$. In road condition b), the PPFs are set as $\varphi_1(t) = (0.1 - 0.002)e^{-3.5t} + 0.002, \varphi_2(t) = (0.1 - 0.05)e^{-8t} + 0.05, \quad \varphi_3(t) = (0.3 - 0.01)e^{-4t} + 0.01$ and other parameters are $k_1 = 0.08, k_2 = 0.05, k_3 = 0.001$. The motivation for using different PPF parameters is to achieve a better control response corresponding to different road conditions. However, the only requirement on the selection of PPF parameters is to fulfill the initial conditions $-\underline{\delta}\varphi_i(t) < e_i(t) < \bar{\delta}\varphi_i(t), \quad \forall t > 0$. In some practical applications, the initial system state may not be measurable or available, which may lead to potential issues. However, this initial condition can still be guaranteed by setting sufficiently large φ_{i0} and $\underline{\delta}, \bar{\delta}$, if the initial system state cannot be precisely measured. Hence, from theoretical analysis point of view, we can set the same parameters for different road conditions. To show the effect of sensor noise, we manually add a band-limited white noise to the measured acceleration $\dot{x}_2$ in the simulations.

Figs. 3–7 show the comparative simulation results. Fig. 3 shows the time domain responses under two different road conditions with three control methods, e.g., the proposed AFC, backstepping control method (BSC) [26], and adaptive control with radical basis function neural network (RBFNN) [11].

From Fig. 3, we can find that the proposed AFC performs superiorly over BSC and RBFNN in terms of a transient suspension response in the time domain. In particular, a slightly faster transient response of AFC can be observed. It is also noted that the RBFNN has more sluggish responses than the other two controllers because the online learning of NNs needs some time to achieve convergence. Nevertheless, the system dynamics are all assumed to be precisely known in the backstepping controller design, which is stringent in practice.

It is also claimed that the AFC method has the reduced computational costs than the other two control methods. To show the improved computational burden, the computational time for simulations of three different methods is presented in Fig. 4. Compared to backstepping method and RBFNN method, we can see that the computational time of the AFC method is dramatically decreased, because the encountered "explosion of complexity" issue can be remedied by using the AFC method and the online calculation of the derivatives of the virtual control signals in backstepping control is avoided in AFC. To be more specific, the overall computational time of AFC compared to backstepping control can be reduced by 76.1% and 79.7% for road conditions a) and b), respectively. Moreover, the decreased convergent time of AFC (i.e., the time required for the vehicle displacement to converge from initial value 0.06 cm to a small set of its final value 0 cm) can also be observed in Fig. 4. This implies that the vehicle motion can be regulated to a small set around zero (i.e., 9×10^{-4}) faster than backstepping control and RBFNN control. Nevertheless, RBFNN control needs longer time to achieve convergence (also shown in Fig. 4) as the

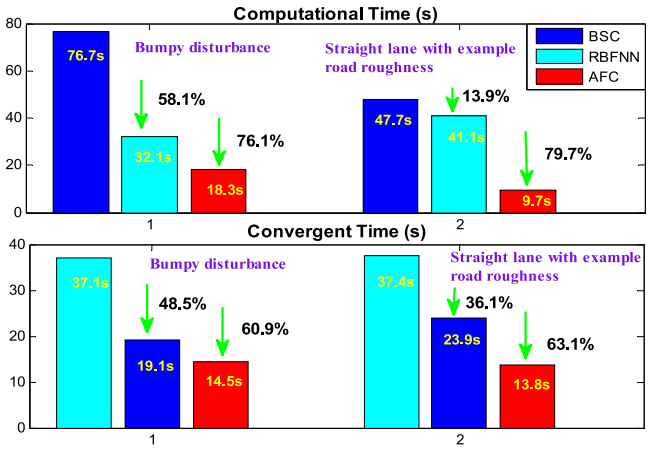

Fig. 4. Comparative computational time.

TABLE I
ACCELERATION RMS (ACC RMS) OF DIFFERENT CONTROLLERS

Methods	Bumpy disturbance	Straight lane with example road roughness
RBFNN	0.9 m/s^2	0.6 m/s^2
BSC	0.42 m/s^2	0.28 m/s^2
AFC	0.3 m/s^2	0.144 m/s^2

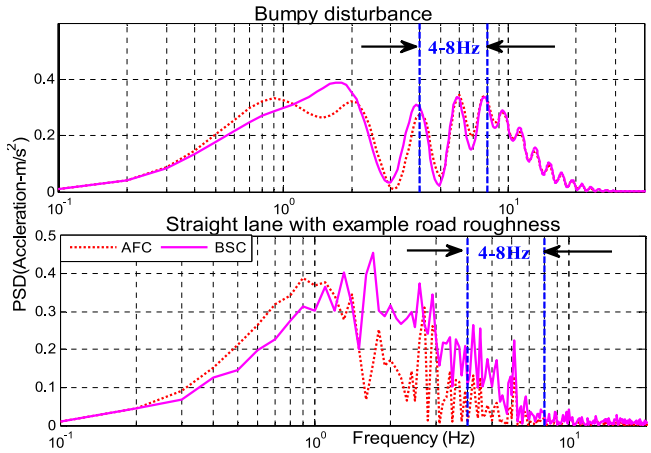

Fig. 5. Frequency analysis for different road conditions.

online learning of the NNs needs a fairly long period to achieve convergence.

On the other hand, the acceleration of suspension motion has been well-recognized as a critical performance index [6], [8], whose magnitude directly reflects the ride comfort of passengers/driver. To quantitatively show the improved response of AFC, the performance index of acceleration root mean square (ACC RMS) of the above-mentioned three controllers is also calculated and shown in Table I. It indicates that the AFC method has the smallest ACC RMS under two load conditions, which indicates that AFC provides better ride comfort.

To further confirm the effectiveness of AFC, the suspension response of a vehicle body in the frequency domain is shown in Fig. 5, which indicates the power spectral density of the acceleration in the vertical direction. One may find from the top

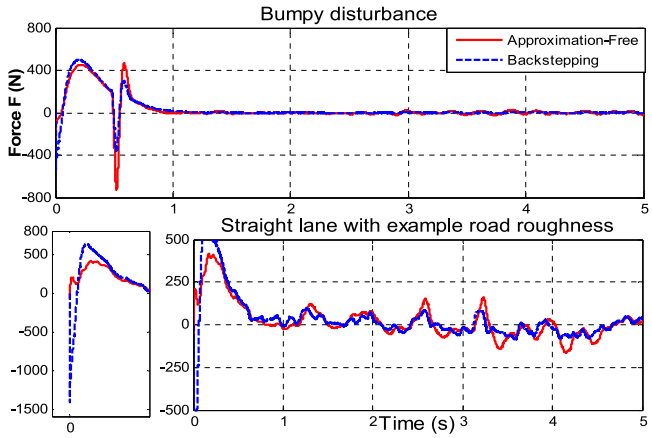

Fig. 6. Profiles of the required control forces.

figure in Fig. 5 that the proposed AFC method can achieve a similar result compared with the backstepping method under road condition a). However, under road condition b), the AFC significantly diminishes the energy compared with that of the backstepping method within the resonant frequency domain (i.e., it is usually limited by the frequency range 4–8 Hz, to which the human body is more sensitive [27]). This implies that the AFC method can provide better riding comfort than the backstepping algorithm.

The actuator forces that are generated by the hydraulic actuator are shown in Fig. 6, where the top figure shows that both the two control methods can guarantee that the required forces are within an acceptable boundary [6], [9]. In the first few seconds around the bumpy road disturbance, AFC has slightly higher peaks than the backstepping method. This phenomenon can be related to the top figure in Fig. 3, in which the vehicle motion with the AFC method has lower peaks and faster convergence rate; therefore, larger control force has to be required for this bumpy road condition. One can also find from the bottom figure in Fig. 6 that there is an aggressive force peak encountered in the initial stage of backstepping control. This is because the derivatives of the virtual control signals should be calculated and used in the backstepping control implementation, which leads to large peaks in the required control actions.

Finally, to ensure the ride safety as stated in Section III-C, the ratio between the tire dynamic load should be always less than 1 and the suspension deflection should be guaranteed within the acceptable range, i.e., $|z_s - z_u| \leq 0.15\,\mathrm{m}$. For road condition b), both the requirements can be strictly guaranteed using the AFC and backstepping method, as shown in Fig. 7. Moreover, a spider chart with more performance indices is shown in Fig. 7 for the straight lane with normal road roughness case, where the maximum two suspension indices shown in Section III-C, the maximum control force, and the maximum motion acceleration and its RMS with different methods are shown. One can see from Fig. 7 that the proposed AFC can help improve the ride comfort (i.e., it has the smallest RMS$(\|\ddot{z}_s\|) = 0.144\,\mathrm{m/s^2}$), reduces the energy consumption (i.e., it requires the smallest $F = 414$ N), and guarantees acceptable suspension deflection. This is due to the fact that the AFC method can guarantee a smoother transient suspension response, and thus, it can effectively manage the

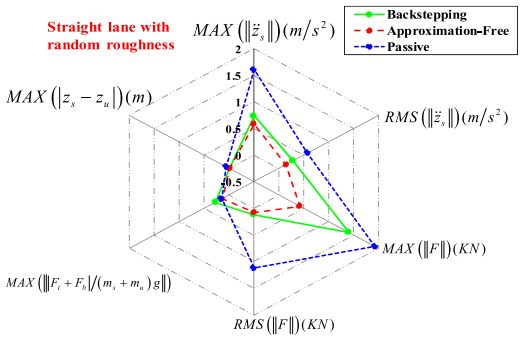

Fig. 7. Comparative control performance results.

tradeoff between the ride comfort and suspension deflection. A similar result can also be observed for the bumpy road condition, which is not provided due to page limitations.

V. Conclusion

In this paper, a novel control strategy was proposed for active suspension systems with unknown nonlinearities, where the widely used function approximation techniques are not needed. Unlike most existing results, we took the hydraulic actuator that creates forces required for active suspension into consideration. Hence, an AFC method was developed based on a systematic design and PPF methodology. Consequently, the heavy computational burden and potential sluggish response due to the online learning of NNs and FLSs were remedied. Moreover, both the transient and steady-state suspension performance was strictly guaranteed. The closed-loop stability was proved, and the suspension requirements were all investigated. The validity of the proposed approach was illustrated in terms of comparative simulations, which were carried out based on a realistic dynamic simulator built in professional vehicle simulation software Carsim. Future work will focus on practical validations of the proposed AFC control strategy in terms of a quarter-car active suspension test-rig with hydraulic actuators.

Appendix
Proof of Theorem 2

Proof: The proof has been inspired by [16]. Based on the intermediate controller errors and its associated normalized errors $\zeta_i(t)$, the state variables x_1, x_2, and x_5 defined in (13)–(23) can be rewritten as

$$x_1 = \zeta_1\varphi_1, \quad x_2 = \zeta_2\varphi_2 + u_1, \quad x_5 = \zeta_3\varphi_3 + u_2. \tag{36}$$

By substituting (36) into (7), the derivatives $\dot{x}_1, \dot{x}_2$, and $\dot{x}_5$ can be reformulated as

$$\begin{cases} \dot{x}_1 = x_2 \\ \dot{x}_2 = \frac{1}{m_s}(-F_d(\zeta_2\varphi_2 + u_1, x_4) - F_s(\zeta_1\varphi_1, x_3) \\ \qquad +\frac{A}{\mu}(\zeta_3\varphi_3 + u_2)) + d_1 \\ \dot{x}_5 = -\beta(\zeta_3\varphi_3 + u_2) - \mu a A(\zeta_2\varphi_2 + u_1 - x_4) + \mu\gamma\omega_3 u \end{cases}. \tag{37}$$

Hence, the derivatives of the normalized error $\zeta_i(t)$ with respect to time t can be calculated along (36) and (37) as

$$\begin{aligned} \dot{\zeta}_1 &= \frac{d(x_1/\varphi_1)}{dt} = \frac{1}{\varphi_1}(\dot{x}_1 - \zeta_1\dot{\varphi}_1) = \frac{1}{\varphi_1}(\zeta_2\varphi_2 + u_1 - \zeta_1\dot{\varphi}_1) \\ &= \nu_1(t, \zeta_1, \zeta_2) \end{aligned} \tag{38}$$

$$\begin{aligned} \dot{\zeta}_2 &= \frac{d(e_2/\varphi_2)}{dt} = \frac{1}{\varphi_2}(\dot{e}_2 - \zeta_2\dot{\varphi}_2) = \frac{1}{\varphi_2}(\dot{x}_2 - \dot{u}_1 - \zeta_2\dot{\varphi}_2) \\ &= \frac{1}{\varphi_2}\left[\frac{1}{m_s}(-F_d(\zeta_2\varphi_2 + u_1, x_4) - F_s(\zeta_1\varphi_1, x_3) \right. \\ &\quad \left. + \frac{A}{\mu}(\zeta_3\varphi_3 + u_2)) + d_1 - \dot{u}_1 - \zeta_2\dot{\varphi}_2\right] \\ &= \nu_2(t, \zeta_1, \zeta_2, \zeta_3) \end{aligned} \tag{39}$$

$$\begin{aligned} \dot{\zeta}_3 &= \frac{d(e_3/\varphi_3)}{dt} = \frac{1}{\varphi_3}(\dot{e}_3 - \zeta_3\dot{\varphi}_3) = \frac{1}{\varphi_3}(\dot{x}_5 - \dot{u}_2 - \zeta_3\dot{\varphi}_3) \\ &= \frac{1}{\varphi_3}[-\beta(\zeta_3\varphi_3 + u_2) - \mu a A(\zeta_2\varphi_2 + u_1 - x_4) \\ &\quad + \mu\gamma\omega_3 u - \dot{u}_2 - \zeta_3\dot{\varphi}_3] \\ &= \nu_3(t, \zeta_2, \zeta_3). \end{aligned} \tag{40}$$

By defining the normalized error vector as $\zeta = [\zeta_1, \zeta_2, \zeta_3]^T$, then (38)–(40) can be rewritten as

$$\dot{\zeta}(t) = \nu(t, \zeta) = \begin{bmatrix} \nu_1(t, \zeta_1, \zeta_2) \\ \nu_2(t, \zeta_1, \zeta_2, \zeta_3) \\ \nu_3(t, \zeta_2, \zeta_3) \end{bmatrix}. \tag{41}$$

In what follows, the proof of Theorem 2 will be conducted in three steps. First, we will prove the existence of maximal solution of (41) over a nonempty and open set as $\Omega_\zeta = (-\underline{\delta}, \bar{\delta}) \times (-\underline{\delta}, \bar{\delta}) \times (-\underline{\delta}, \bar{\delta})$ using Theorem 1. Second, we prove that for all $t \in [0, \tau_{\max})$, the proposed control actions (16), (21), and (25) guarantee all signals in the closed-loop system are bounded. Finally, we will prove the condition $\tau_{\max} = +\infty$ is true by using Proposition 1.

Phase A: The performance functions $\varphi_i(t)$ are selected such that $\varphi_i(0) > \min\{\underline{\delta}, \bar{\delta}\}|e_i(0)|, \quad i = 1, 2, 3$ holds, which implies $|\zeta_i(0)| < \min\{\underline{\delta}, \bar{\delta}\}, \quad i = 1, 2, 3$, i.e., $\zeta(0) \in \Omega_\zeta$ is true for (41). Furthermore, the function $\nu(t, \zeta)$ in (41) is piecewise continuous on t and locally Lipschitz on any ζ over the set Ω_ζ, because the suspension system dynamics in (7) and the performance functions φ_i are all continuous and differentiable with respect to their coordinates. Therefore, the conditions in Theorem 1 are all fulfilled, and thus, there exists a maximal solution $\zeta(t)$ of (41) on a time interval $[0, \tau_{\max})$ such that $\zeta(t) \in \Omega_\zeta$, i.e., $\zeta(t)$ is bounded by $|\zeta_i(t)| < \min\{\underline{\delta}, \bar{\delta}\}, \quad i = 1, 2, 3\ \forall t \in [0, \tau_{\max})$.

Phase B: In this step, we will prove that all signals in the closed-loop system are bounded for $t \in [0, \tau_{\max})$. In this case, the time derivative of ε_1 can be calculated along (15) as

$$\dot{\varepsilon}_1 = \frac{\partial S^{-1}}{\partial \zeta_1}\dot{\zeta}_1 = r_1(\dot{x}_1 - \zeta_1\dot{\varphi}_1) \tag{42}$$

where $r_1 = 1/(2\varphi_1)[1/(\zeta_1+\underline{\delta}) - 1/(\zeta_1-\bar{\delta})]$ fulfills $0 < r_1 \le r_{M1}$ for a positive constant $r_M > 0$ [15].

We substitute $\dot{x}_1 = x_2 = \zeta_2\varphi_2 + u_1$ in (36) into (42), and have

$$\dot{\varepsilon}_1 = r_1(\zeta_2\varphi_2 + u_1 - \zeta_1\dot{\varphi}_1). \tag{43}$$

By applying similar mathematical manipulations as (43) for ε_2 in (20) and ε_3 in (24), we can further obtain

$$\dot{\varepsilon}_2 = \frac{\partial S^{-1}}{\partial\zeta_2}\dot{\zeta}_2 = r_2\left[\frac{1}{m_s}(-F_d(\zeta_2\varphi_2+u_1,x_4) - F_s(\zeta_1\varphi_1,x_3) + \frac{A}{\mu}\zeta_3\varphi_3) + d_1 + \frac{A}{\mu m_s}u_2 - \dot{u}_1 - \zeta_1\dot{\varphi}_1\right] \tag{44}$$

$$\dot{\varepsilon}_3 = \frac{\partial S^{-1}}{\partial\zeta_3}\dot{\zeta}_3 = r_3[-\beta(\zeta_3\varphi_3+u_2) - \mu aA(\zeta_2\varphi_2+u_1-x_4) + \mu\gamma\omega_3 u - \dot{u}_2 - \zeta_3\dot{\varphi}_3] \tag{45}$$

where the positive variables $r_2 = 1/(2\varphi_2)[1/(\zeta_2+\underline{\delta}) - 1/(\zeta_2-\bar{\delta})]$ and $r_3 = 1/2\varphi_3[1/(\zeta_3+\underline{\delta}) - 1/(\zeta_3-\bar{\delta})]$ fulfill $0 < r_i \le r_{Mi}$ for positive constants r_{Mi}.

We choose a Lyapunov function as

$$V_1 = \frac{1}{2}\varepsilon_1^2. \tag{46}$$

Then the time derivate of V_1 can be obtained along (43) as

$$\dot{V}_1 = \varepsilon_1\dot{\varepsilon}_1 = \varepsilon_1 r_1(\zeta_2\varphi_2 - \zeta_1\dot{\varphi}_1 - k_1\varepsilon_1). \tag{47}$$

Consider $|\zeta_i(t)| < \min\{\underline{\delta},\bar{\delta}\}, \quad \forall t\in[0,\tau_{\max})$ and φ_2 and $\dot{\varphi}_1$ are all bounded, then based on the extreme value theorem [25], we know that there exists a positive constant $F_1 > 0$, such that

$$|\zeta_2\varphi_2 - \zeta_1\dot{\varphi}_1| \le F_1, \quad \text{for } \forall t\in[0,\tau_{\max}). \tag{48}$$

Thus, one can obtain from (47) to (48)

$$\dot{V}_1 \le |\varepsilon_1|\, r_{M1}\,(F_1 - k_1\,|\varepsilon_1|). \tag{49}$$

One may verify from (49) that $\dot{V}_1$ is negative for any $|\varepsilon_1| > F_1/k_1$. Then, it follows from the Lyapunov theorem that ε_1 will converge to a compact set $\Omega_1 := \{\varepsilon_1 \| \varepsilon_1| \le \varepsilon_{M1}\}$ with $\varepsilon_{M1} = \max\{|\varepsilon_1(0)|, F_1/k_1\}$ for $\forall t\in[0,\tau_{\max})$. Then, one can claim that the intermediate controller $u_1 = -k_1\varepsilon_1$ given in (16) and its derivative are bounded, and $\dot{\varepsilon}_1$ is also bounded from (42), i.e., $\varepsilon_1, u_1, \dot{\varepsilon}_1, \dot{u}_1 \in L_\infty$ for $t\in[0,\tau_{\max})$. Moreover, from Lemma 1, we know $-\underline{\delta}\varphi_1(t) < x_1(t) < \bar{\delta}\varphi_1(t)$ holds, so that the vertical motion x_1 with prescribed bound (9) is achieved.

Similarly, we select a Lyapunov function as $V_2 = 1/2\varepsilon_2^2$, then its time derivative can be derived along (44) as

$$\begin{aligned}\dot{V}_2 &= \varepsilon_2 r_2[(-F_d(\zeta_2\varphi_2+u_1,x_4) - F_s(\zeta_1\varphi_1,x_3) + A\zeta_3\varphi_3/\mu)/m_s - \dot{u}_1 - \zeta_2\dot{\varphi}_2 + d_1 - Ak_2\varepsilon_2/\mu m_s] \\ &\le |\varepsilon_2|\, r_{M2}\,[F_2 - k_2 A\theta_{\min}\,|\varepsilon_2|\,/\mu + d_m]\end{aligned} \tag{50}$$

where the positive constant $F_2 > 0$ represents the upper bound of $|\frac{1}{m_s}(-F_d(\zeta_2\varphi_2+u_1,x_4) - F_s(\zeta_1\varphi_1,x_3) + \frac{A}{\mu}\zeta_3\varphi_3) - \dot{u}_1 - \zeta_2\dot{\varphi}_2| \le F_2 \quad \forall t\in[0,\tau_{\max})$, which can be verified using the extreme value theorem because $|\zeta_2(t)| < \min\{\underline{\delta},\bar{\delta}\}$ and $\varphi_2, \dot{\varphi}_2, \varphi_1$, and $\dot{u}_1$ are all bounded. In this case, we can claim from (50) that ε_2 will converge to a compact set $\Omega_2 := \{\varepsilon_2 \| \varepsilon_2| \le \varepsilon_{M2}\}$ with $\varepsilon_{M2} = \max\{|\varepsilon_2(0)|, \mu(F_2+d_m)/(k_2 A\theta_{\min})\}$. Thus, the intermediate controller u_2 and its time derivative $\dot{u}_2$ are also bounded. Furthermore, according to Lemma 1, we can conclude that the intermediate controller error $e_2(t)$ can be guaranteed within the bound, and the state x_2 is bounded for $t\in[0,\tau_{\max})$.

Finally, by considering $V_3 = 1/2\varepsilon_3^2$, we have $\dot{V}_3$ along (45)

$$\begin{aligned}\dot{V}_3 &= \varepsilon_3 r_3[-\beta(\zeta_3\varphi_3+u_2) - \mu aA(\zeta_2\varphi_2+u_1-x_4) + \mu\gamma\omega_3 u - \dot{u}_2 - \zeta_3\dot{\varphi}_3] \\ &\le |\varepsilon_3|\, r_{M3}\,[F_3 - \mu\gamma\omega_3 k_3\,|\varepsilon_3|]\end{aligned} \tag{51}$$

where the positive constant $F_3 > 0$ denotes the upper bound of $|-\beta(\zeta_3\varphi_3+u_2) - \mu aA(\zeta_2\varphi_2+u_1-x_4) - \dot{u}_2 - \zeta_3\dot{\varphi}_3| \le F_3 \quad \forall t\in[0,\tau_{\max})$. This can be illustrated in terms of applying the extreme value theorem, and the facts $|\zeta_3(t)| < \min\{\underline{\delta},\bar{\delta}\}$ and $\varphi_2, \varphi_3, \dot{\varphi}_3$, and $\dot{u}_2$ are all bounded. Therefore, we conclude from (51) that ε_3 will converge to a compact set $\Omega_3 := \{\varepsilon_3 \| \varepsilon_3| \le \varepsilon_{M3}\}$ for $\varepsilon_{M3} = \max\{|\varepsilon_3(0)|, F_3/(\mu\gamma\omega_3 k_3)\}$, and thus, the control signal $u = -k_3\varepsilon_3$ and the state x_5 are bounded for $t\in[0,\tau_{\max})$.

Phase C: Finally, we need to show that $\tau_{\max} = +\infty$ by deriving a contradiction. From Lemma 1 and (27), the condition $\zeta(t)\in\bar{\Omega}_\zeta \quad \forall t\in[0,\tau_{\max})$ is true for a set defined by $\bar{\Omega}_\zeta = \prod_{i=1}^{3}[\frac{e^{-\varepsilon_M i}\bar{\delta}-\underline{\delta}}{e^{-\varepsilon_M i}+1}, \frac{e^{\varepsilon_M i}\bar{\delta}-\underline{\delta}}{e^{\varepsilon_M i}+1},]$, which is a nonempty and compact open set. Clearly, it can be verified that $\bar{\Omega}_\zeta \subset \Omega_\zeta$ with $\Omega_\zeta = (-\underline{\delta},\bar{\delta})\times(-\underline{\delta},\bar{\delta})\times(-\underline{\delta},\bar{\delta})$. Hence, if we assume $\tau_{\max} < +\infty$, then Proposition 1 indicates that there exists a time instant $t_1\in[0,\tau_{\max})$ such that $\zeta(t_1)\notin\bar{\Omega}_\zeta$. This clearly creates a contradiction. Consequently, the opposite of the assumption is true, that is, $\tau_{\max} = +\infty$. To this end, we can claim that all signals in the closed-loop systems are bounded and the vertical motion x_1 can be retained within the prescribed bound (9) for all $t \ge 0$. This completes the proof. ♢

REFERENCES

[1] D. Cao, X. Song, and M. Ahmadian, "Editors' perspectives: Road vehicle suspension design, dynamics, and control," *Veh. Syst. Dyn.*, vol. 49, nos. 1–2, pp. 3–28, 2011.

[2] N. Yagiz, Y. Hacioglu, and Y. Taskin, "Fuzzy sliding-mode control of active suspensions," *IEEE Trans. Ind. Electron.*, vol. 55, no. 11, pp. 3883–3890, Nov. 2008.

[3] D. Hrovat, "Survey of advanced suspension developments and related optimal control applications," *Automatica*, vol. 33, no. 10, pp. 1781–1817, 1997.

[4] J. J. Rath, M. Defoort, H. R. Karimi, and K. C. Veluvolu, "Output feedback active suspension control with higher order terminal sliding mode," *IEEE Trans. Ind. Electron.*, vol. 64, no. 2, pp. 1392–1403, Feb. 2017.

[5] Y. Huang, J. Na, X. Wu, X. Liu, and Y. Guo, "Adaptive control of nonlinear uncertain active suspension systems with prescribed performance," *ISA Trans.*, vol. 54, pp. 145–155, 2015.

[6] W. Sun, Y. Zhao, J. Li, L. Zhang, and H. Gao, "Active suspension control with frequency band constraints and actuator input delay," *IEEE Trans. Ind. Electron.*, vol. 59, no. 1, pp. 530–537, Jan. 2012.

[7] W. Sun, H. Gao, and O. Kaynak, "Adaptive backstepping control for active suspension systems with hard constraints," *IEEE/ASME Trans. Mechatron.*, vol. 18, no. 3, pp. 1072–1079, Jun. 2013.

[8] H. Chen and K.-H. Guo, "Constrained H_∞ control of active suspensions: An LMI approach," *IEEE Trans. Control Syst. Technol.*, vol. 13, no. 3, pp. 412–421, May 2005.

[9] G. Koch and T. Kloiber, "Driving state adaptive control of an active vehicle suspension system," *IEEE Trans. Control Syst. Technol.*, vol. 22, no. 1, pp. 44–57, Jan. 2014.
[10] K. Nakano, Y. Suda, and S. Nakadai, "Self-powered active vibration control using a single electric actuator," *J. Sound Vib.*, vol. 260, no. 2, pp. 213–235, 2003.
[11] F. Zhao, S. S. Ge, F. Tu, Y. Qin, and M. Dong, "Adaptive neural network control for active suspension system with actuator saturation," *IET Control Theory Appl.*, vol. 10, no. 14, pp. 1696–1705, 2016.
[12] H. Li, J. Yu, C. Hilton, and H. Liu, "Adaptive sliding-mode control for nonlinear active suspension vehicle systems using T–S fuzzy approach," *IEEE Trans. Ind. Electron.*, vol. 60, no. 8, pp. 3328–3338, Aug. 2013.
[13] C. P. Bechlioulis and G. A. Rovithakis, "Adaptive control with guaranteed transient and steady state tracking error bounds for strict feedback systems," *Automatica*, vol. 45, no. 2, pp. 532–538, 2009.
[14] J. Na, "Adaptive prescribed performance control of nonlinear systems with unknown dead zone," *Int. J. Adapt. Control Signal Process.*, vol. 27, no. 5, pp. 426–446, 2013.
[15] J. Na, Q. Chen, X. Ren, and Y. Guo, "Adaptive prescribed performance motion control of servo mechanisms with friction compensation," *IEEE Trans. Ind. Electron.*, vol. 61, no. 1, pp. 486–494, Jan. 2014.
[16] C. P. Bechlioulis and G. A. Rovithakis, "A low-complexity global approximation-free control scheme with prescribed performance for unknown pure feedback systems," *Automatica*, vol. 50, no. 4, pp. 1217–1226, 2014.
[17] H. Du and N. Zhang, "Fuzzy control for nonlinear uncertain electrohydraulic active suspensions with input constraint," *IEEE Trans. Fuzzy Syst.*, vol. 17, no. 2, pp. 343–356, Apr. 2009.
[18] J. Lin and R.-J. Lian, "Intelligent control of active suspension systems," *IEEE Trans. Ind. Electron.*, vol. 58, no. 2, pp. 618–628, Feb. 2011.
[19] I. Fialho and G. J. Balas, "Road adaptive active suspension design using linear parameter-varying gain-scheduling," *IEEE Trans. Control Syst. Technol.*, vol. 10, no. 1, pp. 43–54, Jan. 2002.
[20] W. Sun, H. Pan, Y. Zhang, and H. Gao, "Multi-objective control for uncertain nonlinear active suspension systems," *Mechatronics*, vol. 24, no. 4, pp. 318–327, 2014.
[21] A. Alleyne, P. Neuhaus, and J. Hedrick, "Application of nonlinear control theory to electronically controlled suspensions," *Veh. Syst. Dyn.*, vol. 22, nos. 5–6, pp. 309–320, 1993.
[22] H. E. Merritt, *Hydraulic Control Systems*. Hoboken, NJ, USA: Wiley, 1967.
[23] R. Rajamani and J. K. Hedrick, "Adaptive observers for active automotive suspensions: Theory and experiment," *IEEE Trans. Control Syst. Technol.*, vol. 3, no. 1, pp. 86–93, Mar. 1995.
[24] E.-S. Kim, "Nonlinear indirect adaptive control of a quarter car active suspension," in *Proc. 1996 IEEE Int. Conf. Control Appl.*, 1996, pp. 61–66.
[25] E. D. Sontag, *Mathematical Control Theory*. London, U.K.: Springer, 1998.
[26] S. S. Ge and C. Wang, "Direct adaptive NN control of a class of nonlinear systems," *IEEE Trans. Neural Netw.*, vol. 13, no. 1, pp. 214–221, Jan. 2002.
[27] H. Li, X. Jing, and H. R. Karimi, "Output-feedback-based control for vehicle suspension systems with control delay," *IEEE Trans. Ind. Electron.*, vol. 61, no. 1, pp. 436–446, Jan. 2014.

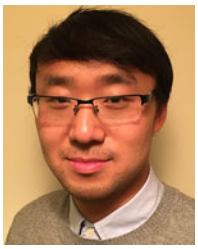

Yingbo Huang received the B.Sc. degree in mechanical design, manufacturing and automation from Lanzhou City University, Lanzhou, China, in 2013. He is working toward the Ph.D. degree in mechanical & electronic engineering with the Kunming University of Science and Technology, Kunming, China.

His current research interests include adaptive control and transient performance improvement with application to vehicle suspension systems.

Jing Na (M'15) received the B.Sc. degree in automation and Ph.D. degree in dynamics and control from the School of Automation, Beijing Institute of Technology, Beijing, China, in 2004 and 2010, respectively.

From 2011 to 2013, he was a Monaco/ITER Postdoctoral Fellow with the ITER Organization Saint-Paul-lès-Durance, France. From 2015 to 2017, he was a Marie Curie Intra-European Fellow with the Department of Mechanical Engineering, University of Bristol, Bristol, U.K. Since 2010, he has been with the Faculty of Mechanical and Electrical Engineering, Kunming University of Science and Technology, Kunming, China, where he became a Professor in 2013. His current research interests include intelligent control, adaptive parameter estimation, neural networks, repetitive control, and nonlinear control and applications.

Dr. Na was a recipient of the Best Application Paper Award of the third IFAC International Conference on Intelligent Control and Automation Science, and 2017 Hsue-shen Tsien Paper Award.

Xing Wu received the B.Sc. and M.Sc. degrees in mechanical engineering from Kunming University of Science and Technology, Kunming, China, in 1994 and 1997, respectively, and the Ph.D. degree in mechanical design & theory from Shanghai Jiao Tong University, Shanghai, China, in 2005.

He is currently a Professor with the Faculty of Mechanical and Electrical Engineering, Kunming University of Science and Technology. His current research interests include modern signal processing theory and their applications on fault feature extracting, and internet-based mechanical fault diagnosis technology and expert systems.

Guanbin Gao received the B.Sc. and M.Sc. degrees in mechanical engineering and automation from Northeastern University, Shenyang, China, in 2001 and 2004, respectively, and the Ph.D. degree in mechanical manufacturing and automation from Zhejiang University, Hangzhou, China, in 2010.

His current research interests include precision measuring and control, kinematics of industrial robots, and neural networks.